ETH zürich

Theory Group
Trapped Ion Quantum Information

Partial permutational symmetry in bipartite systems

Semester project

Marcello Massimo Negri

3rd semester M. Sc. in Physics
mnegri@student.ethz.ch

Supervised by
Dr. Florentin Reiter

Co-supervised by
Dr. Thanh Long Nguyen

Abstract: Several physical systems of interest consist of an ensemble of two-level systems coupled to a bosonic mode in an open system setting. Therefore, it is fundamental to be able to efficiently simulate such quantum systems in order to test hypothesis and make predictions. When all two-level systems are assumed to be identical, the permutational symmetry of the ensemble allows to exponentially reduce the computational resources needed. This powerful result has been implemented in the open source library *Permutational Invariant Quantum Solver* and has been successfully applied to explore a wide variety of physical phenomena such as superradiant light emission, spin squeezing, phase transitions, and the ultrastrong coupling regime. As soon as a one two-level system can be distinguished from the others though, the permutational symmetry is broken and the exponential complexity is recovered. In this project we explore how to extend the applicability of PIQS to mixed-species ensembles characterised by *partial* permutational symmetry and if this can be done with the same exponential reduction of computational resources. In particular, we focus on the case of a bipartite system composed of two-level systems belonging to two different species. This example allows to show that the speedup is still substantial and gives a way to estimate the complexity for a more general mixed-species scenario, which is of great scientific interest.

Zürich

Winter semester 2021

Contents

1 Introduction

The building block of this work is the two-level system (TLS), which is the simplest and yet most fundamental quantum model. When the system is coupled to an electromagnetic environment, its dynamics allows to investigate a wide range of physical phenomena. Of particular interest is the case of an ensemble of many TLSs interacting with a single mode of a harmonic oscillator because it allows to describe the interaction between light and matter. This model, known as the Dicke model, has received particular attention as it reveals a peculiar phase transition to a superradiant state [1]. In its simplest implementation the model assumes the system to be perfectly isolated from the environment but in actual laboratories this assumption does not hold in general. As a matter of fact, quantum coherence is easily affected by uncontrolled interactions with the environment and the unitary evolution of the system is thus lost. In order to describe the dynamics of such an open quantum system, the Born-Markov approximation is usually exploited to obtain the associated master equation. However, to describe the ensemble of TLSs under study the solutions require exponential resources, which makes computational simulations unfeasible already for very few TLSs. One way to reduce the complexity of the problem is to assume identical TLSs and to exploit the resulting permutational invariance of the master equation. This possibility has been studied and recently implemented in an open-source library named *Permutational Invariant Quantum Solver* (PIQS) [2], which is meant for simulating open quantum systems and is integrated in the widely used QuTiP library [3]. Other authors have proposed different solutions that provide an exponential speed up, such as the *Permutation symmetry for identical Quantum Systems Package* (PsiQuaSP) [4]. The latter is an open-source library that allows to study the interaction between multi-level systems, hence beyond the TLSs model, and bosonic fields. On the one hand, the PIQS solution to the problem is to choose as state basis one that already assumes the permutational invariance of the system. On the other, the approach followed by PsiQuaSP is numerical, as it exploits matrix multiplication techniques that take into account the symmetry of the problem in order to efficiently solve the differential equations. In other words, it could be argued that the first approach is *a priori*, assuming the symmetry of the problem, while the second is *a posteriori*, exploiting the symmetry of the problem.

In this work we decided to focus on the PIQS method. The PIQS correctness and performance have been widely validated for single species scenarios such as superradiant light emission [5], steady-state superradiance [6], spin squeezing [7], phase transitions [8] and ultrastrong-coupling regime [9], each scenario being separately addressed in a dedicated jupyter notebook [10]. Multi-spin ensembles have been studied in the context of Dicke model but only in a specific bad-cavity limit, where the harmonic oscillator degree of freedom can be traced out [11]. However, the case of multi-spin ensemble has been of great interest, especially in recent applications such as atom synchronization [12] or quantum information processing protocols [13], and many others. Mixed-species spin-boson models have been proven to be implementable in trapped ion setups [14] as well. This work explores the possibility of extending the applicability of the PIQS assumptions of permutational symmetry to partial permutational symmetry in mixed-species ensembles. The focus is put on studying the simpler two-species scenario as it allows to draw conclusions that can be easily generalised to multi-species scenarios. In Figure 1 we report a graphical illustration of a spin-boson model in the mixed species scenario in the case of two different species.

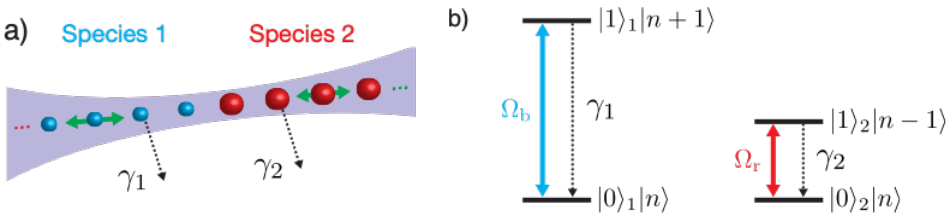

Figure 1: Graphical illustration of the spin-boson model in the mixed species scenario where two species are present. On the left, the two species are represented in blue and red, characterized by their decay rates γ_1 and γ_2. On the right, the diagram of the corresponding two-level systems is reported.

2 Physical system and permutational symmetry

The simplest ensemble that is considered in this project is composed of N identical TLSs and will be referred to as the single species case. This system, which has been widely studied, can be simulated

efficiently by exploiting the permutational invariance of the identical TLSs. This idea has already been implemented in the PIQS library and validated in different setups. Nonetheless, it is still instructive to go through the main concepts and ideas in order to investigate the biparite system scenario and, ultimately, to go beyond the single species case.

2.1 Single species case

Let us consider an open quantum system consisting of N identical TLSs. Its dynamics is described by the following Lindblad *master equation*:

$$\begin{aligned}\dot{\rho} = &-\frac{i}{\hbar}[H_{\mathrm{TLS}}, \rho] + \frac{\gamma_{\Downarrow}}{2}\mathcal{L}_{J_-}[\rho] + \frac{\gamma_{\Phi}}{2}\mathcal{L}_{J_z}[\rho] + \frac{\gamma_{\Uparrow}}{2}\mathcal{L}_{J_+}[\rho] \\ &+ \sum_{n=1}^{N}\Big(\frac{\gamma_{\downarrow}}{2}\mathcal{L}_{J_{-,n}}[\rho] + \frac{\gamma_{\phi}}{2}\mathcal{L}_{J_{z,n}}[\rho] + \frac{\gamma_{\uparrow}}{2}\mathcal{L}_{J_{+,n}}[\rho]\Big),\end{aligned} \tag{1}$$

where ρ is the density matrix of the full system and H_{TLS} the TLS ensemble Hamiltonian, which may be taken as $H_{\mathrm{TLS}} = \omega_0 J_z + \omega_x J_x$. Here and in the following the notation of the PIQS paper [2] will be used: J_α and $J_{\alpha,n}$ are respectively collective and local spin operators, where $\alpha = \{z, x, +, -\}$. The Lindblad superoperators are defined as $\mathcal{L}_A[\rho] = 2A\rho A^\dagger - A^\dagger A\rho + \rho A^\dagger A$ and γ_i terms represent homogeneous collective decay rate by spontaneous emission ($\gamma_{\Downarrow}$), dephasing (γ_{Φ}), pumping ($\gamma_{\Uparrow}$), and their respective local counterparts ($\gamma_{\downarrow}, \gamma_{\phi}, \gamma_{\uparrow}$).

In order to simulate such a system, it is fundamental to first choose a basis to represent the operators in Eq (1). This is particularly crucial for the resulting computational complexity of the problem. One way to build suitable basis for the system in question is to start by defining the ground state of the system as

$$|0_N\rangle := \bigotimes_{i=1}^{N} |0\rangle_i \,. \tag{2}$$

The excited states, from which the basis is built, can then be constructed from the ground state by applying raising operators. *Local* raising operators, acting on each TLS separately, or alternatively *collective* raising operators, acting simultaneously on all TLSs, may be applied on the ground state $|0_N\rangle$. As a result of this choice, it is possible to obtain different basis representations [15]: the uncoupled basis and the Dicke basis.

2.1.1 Uncoupled basis representation

The entire dynamics of a single TLS can be described by the following four operators:

$$\begin{aligned}\sigma_{11} &= |1\rangle\langle 1|\,, \quad \sigma_{01} = |0\rangle\langle 1|\,, \\ \sigma_{10} &= |1\rangle\langle 0|\,, \quad \sigma_{00} = |0\rangle\langle 0|\,,\end{aligned} \tag{3}$$

where σ_{10} is the individual raising operators. Obviously, these operators can be considered for the general i-th TLSs as $\sigma_{10}^i = |1\rangle_i \langle 0|_i$. The excited state on the i-th TLS can thus be obtained as

$$\sigma_{10}^i |0_N\rangle = |0\rangle_1 \ldots |0\rangle_{i-1} |1\rangle_i |0\rangle_{i+1} \ldots |0\rangle_N \,. \tag{4}$$

Similarly, single excitations can be obtained for each TLS by applying the respective raising operator σ_{10}^i. Higher excited states are obtained by applying the raising operator to n different two-level systems and by doing so the uncoupled basis is built. Clearly, several states have identical excitation energy, hence a degeneracy in energy rises immediately. If n TLSs are excited, the degeneracy of the configuration is given by $D = \binom{N}{n}$. Overall, the total dimension of the Hilbert space described by the uncoupled basis becomes $\dim(\mathcal{H}) = \sum_{n=0}^{N}\binom{N}{n} = 2^N$. This result can also be derived by noting that in the uncoupled basis all possible combinations of excited states are represented. The total number of states is thus given by the power set of the set of N TLSs, which gives exactly 2^N. This is the number of states of the uncoupled basis, which will be referred to as $n_{\mathrm{US}}(N)$. When considering the density matrix ρ in Eq (1), the numerical complexity becomes 4^N, as the number of entries of ρ is the square of the dimension of the Hilbert space. This behaviour is a consequence of simulating an open quantum system, which is more demanding in terms of numerical complexity with respect to its closed counterpart. Relevantly, in terms of computational complexity the main bottleneck is constituted by the dimension of the space used to represent the system, which in this case is exponential in the number of TLSs. This makes the uncoupled basis a feasible representation of the system only for very few TLSs.

2.1.2 Dicke basis representation

Another way to build a basis for an ensemble of N TLSs is to exploit a collective raising operator, in place of the local σ_{10}^i. The former is defined as

$$J_{10} = \sum_{i=1}^{N} \sigma_{10}^i, \tag{5}$$

while J_{00}, J_{01}, and J_{11} can be readily derived by adjusting the indexes accordingly (σ_{00}^i, σ_{01}^i, and σ_{11}^i, respectively). From these operators it is possible to define the collective operators J_z and J^2 as

$$\begin{aligned} J_z &= \frac{1}{2}(J_{11} - J_{00}) \\ J^2 &= \frac{1}{4}(J_{01}J_{10} + J_{10}J_{01}) + J_z^2. \end{aligned} \tag{6}$$

The Dicke basis can then be obtained as the states $|l, m\rangle$ that are simultaneously eigenstates of J_z and J^2:

$$\begin{cases} J^2 |l, m\rangle = l(l+1) |l, m\rangle \\ J_z |l, m\rangle = m |l, m\rangle \end{cases} \tag{7}$$

where $l \leq N/2$ and $|m| < l$. l and m are integers or half-integers depending on whether N is even or odd, respectively. The operators J_{10} and J_{01} can be interpreted as the ladders operators J_+ and J_-, respectively:

$$J_\pm |l, m\rangle = \sqrt{(l \mp m)(l \pm m + 1)}\, |l, m \pm 1\rangle \tag{8}$$

Unfortunately, the calculations needed to explicitly obtain the form of the Dicke state basis are quite cumbersome. One notable exception are the so called *symmetric* Dicke states with $l = N/2$, which can be easily obtained as the symmetric superposition of states with $k \in \{0, .., N\}$ excited TLSs:

$$\left| \frac{N}{2}, k - \frac{N}{2} \right\rangle = \frac{1}{\sqrt{\binom{N}{k}}} \mathcal{S}\big[|e\rangle^{\otimes k} \otimes |g\rangle^{\otimes (N-k)} \big], \tag{9}$$

where $\mathcal{S}$ is the symmetrisation operator. The remaining Dicke states with $l < N$ can be obtained iteratively [16], as in the Clebsch-Gordan coefficients recursive construction. Intuitively, if the permutational invariance of the system is assumed, fewer basis states with respect to the uncoupled basis are needed. This is the case for the Dicke basis. In particular the number of Dicke states n_{DS} for an ensemble of N identical TLSs is given by [2]

$$n_{\mathrm{DS}}(N) = \sum_{l=l_{min}}^{N/2} (2l+1) = \left(\frac{N}{2} + 1 \right)^2 - \frac{N \bmod 2}{4}, \tag{10}$$

where $l_{\min}$ is the minimum value of l, which can be either 0 or 1/2 according to whether N is even or odd, respectively. This constitutes an *exponential reduction* in the number of basis states compared to the 2^N needed in the uncoupled representation. In particular, as a consequence of the permutational invariance of the system, one Dicke basis state may correspond to a superposition of several uncoupled basis states, hence the degeneracy. In particular, it can be computed that the degeneracy d_N^l, associated to the Dicke state $|l, m\rangle$ for a system of N identical TLSs, is equal to $d_N^l = \frac{(2l+1)N!}{(N/2+l+1)!(N/2-l)!}$.

Intuitively, the idea behind using collective operators is that, if the TLSs are assumed to be identical, it is possible to exploit the intrinsic permutational symmetry of the collective operators. This is particularly evident when the dynamics is driven only by collective operators (J^2, $J_\pm$ and J_z). In fact, by looking at Eq. (7) and Eq. (8), it is apparent that l is conserved and, consequently, that the system is split into subspaces of dimension $2l + 1$. In other words, since J^2 commutes with the Hamiltonian and with the operators in the master equation, it constitutes a conserved quantity and l is thus conserved. Nevertheless, if local ($J_{-,n}$, $J_{z,n}$, and $J_{+,n}$) or non-collective spin operators are introduced, l ceases to be a conserved quantity. In particular, it is not apparent how local operators $J_{\alpha,n}$ in Eq. (1) act on the Dicke states, where $\alpha \in \{+, -, z\}$. At this point, the idea is to restrict the analysis to states that are initially prepared through collective operators only, which generate permutational symmetric density matrices. It can be shown [2] that Eq (1) does not create coherences, i.e. elements with $m \neq m'$, between Dicke states with

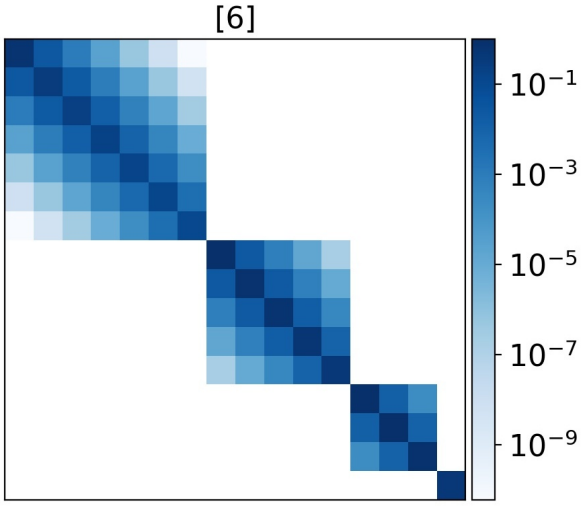

(a) Block-diagonal structure of the density matrix in the Dicke basis for $N = 6$. Each block is uniquely associated to a value of $l \in \{0, 1, 2, 3\}$, which increases from bottom right to top left. The length of each block, in terms of the number of its elements along one edge, is equal to $2l + 1$.

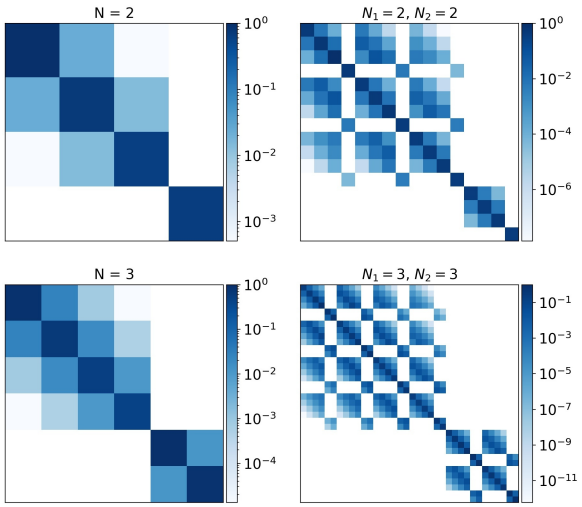

(b) Comparison of block-diagonal structure of the density matrix in the Dicke basis for one-species $N = 2$ (top left) and $N = 3$ (bottom left) and for the bipartite system $N_1 = 2, N_2 = 2$ (top right) and $N_1 = 3, N_2 = 3$ (bottom right). It is interesting to note the fractal-like structure of the bipartite system case.

Figure 2: The plots are obtained by letting the system evolve according to the corresponding master equation Eq. (1) for the one-species case and Eq. (13) for the bipartite system, which results in a sequence of density matrices (one for each time step). Of each element in the matrix the absolute value is taken and is then summed with its homologue in the other matrices in the sequence. The values are finally rescaled in the interval $[0, 1]$. The logarithmic color scale should give an idea of the mean relative abundances of each element of the density matrix during its evolution.

$l \neq l'$. Consequently, the density matrices that describe the system have a block-diagonal structure, as the one illustrated in Figure 2a.

It is now straightforward to compute the total number of elements in the density matrix since each block is associated to a fixed value l and has $(2l + 1)^2$ elements. It is worth noticing that as l decreases, or in other words as the block in the diagonal gets smaller, the degeneracy of the state basis increases. Overall, the total number of elements in the density matrix is given by the following expression:

$$\sum_{l=l_{\min}}^{N/2} (2l + 1)^2 = \frac{1}{6}(N + 1)(N + 2)(N + 3) = O(N^3). \tag{11}$$

This constitutes an *exponential reduction* in the number of elements of the density matrix that must be computed in a simulation, compared to the 4^N elements obtained with the uncoupled basis. This reduction is at the heart of the exponential speedup obtained by the PIQS library.

2.2 Bipartite system

The computational speedup obtained exploiting the Dicke basis is established under the hypothesis that the TLSs in the ensemble are identical. As soon as one TLS can be distinguished from the others, the permutational symmetry is broken and the arguments illustrated do not hold anymore. One could consider using the uncoupled representation but this would recover the initial exponential complexity. One possible solution lies in between the two: In this project, we explore the possibility to use one Dicke basis for each species and to construct a basis for the whole system as tensor product of local Dicke states. For illustrative purposes, only the case of two-species is analysed as multi-species scenarios can be readily generalised from it.

Let's consider an ensemble of N_1 TLSs of one-species and N_2 TLSs of another species and the respective Hamiltonians:

$$\begin{aligned} H^{(1)}_{\text{TLS}} &= \hbar\omega_0^{(1)} J_z^{(1)} + \hbar\omega_x^{(1)} J_x^{(1)}, \\ H^{(2)}_{\text{TLS}} &= \hbar\omega_0^{(2)} J_z^{(2)} + \hbar\omega_x^{(2)} J_x^{(2)}, \end{aligned} \tag{12}$$

where the superscripts $^{(1)}$ and $^{(2)}$ indicate the different species. The dynamics of such a system is described by the following master equation:

$$\begin{aligned}\dot{\rho} = &-\frac{i}{\hbar}[H^{(1)}_{\mathrm{TLS}} + H^{(2)}_{\mathrm{TLS}}, \rho] \\ &+\frac{\gamma^{(1)}_{\Downarrow}}{2}\mathcal{L}_{J^{(1)}_{-}}[\rho] + \frac{\gamma^{(1)}_{\Phi}}{2}\mathcal{L}_{J^{(1)}_{z}}[\rho] + \frac{\gamma^{(1)}_{\Uparrow}}{2}\mathcal{L}_{J^{(1)}_{+}}[\rho] \\ &+\frac{\gamma^{(2)}_{\Downarrow}}{2}\mathcal{L}_{J^{(2)}_{-}}[\rho] + \frac{\gamma^{(2)}_{\Phi}}{2}\mathcal{L}_{J^{(2)}_{z}}[\rho] + \frac{\gamma^{(2)}_{\Uparrow}}{2}\mathcal{L}_{J^{(2)}_{+}}[\rho] \\ &+\sum_{n=1}^{N_1}\frac{\gamma^{(1)}_{\downarrow}}{2}\mathcal{L}_{J^{(1)}_{-,n}}[\rho] + \frac{\gamma^{(1)}_{\phi}}{2}\mathcal{L}_{J^{(1)}_{z,n}}[\rho] + \frac{\gamma^{(1)}_{\uparrow}}{2}\mathcal{L}_{J^{(1)}_{+,n}}[\rho] \\ &+\sum_{n=1}^{N_2}\frac{\gamma^{(2)}_{\downarrow}}{2}\mathcal{L}_{J^{(2)}_{-,n}}[\rho] + \frac{\gamma^{(2)}_{\phi}}{2}\mathcal{L}_{J^{(2)}_{z,n}}[\rho] + \frac{\gamma^{(2)}_{\uparrow}}{2}\mathcal{L}_{J^{(2)}_{+,n}}[\rho],\end{aligned} \tag{13}$$

where $J^{(1/2)}_z$, $J^{(1/2)}_+$, and $J^{(1/2)}_-$ are collective operators acting globally on each species separately. The definition of such collective operators may be adjusted according to the physical problem under study. For instance, two collective operators can be considered separately as $J_z := J^{(1)}_z \otimes \mathbb{1}^{(2)}$ and $J_z := \mathbb{1}^{(1)} \otimes J^{(2)}_z$ or together as $J_z := J^{(1)}_z \otimes \mathbb{1}^{(2)} + \mathbb{1}^{(1)} \otimes J^{(2)}_z$ (and similarly for J_+ and J_-).

On the one hand, if the uncoupled basis is considered, the complexity is still exponential in the number of TLSs of the ensemble. As a matter of fact, the same considerations for the single-species setup illustrated in the previous section hold and can be recovered by simply setting $N = N_1 + N_2$. Consequently, such a system can be simulated for very few TLS, even less TLSs for each species since the complexity depends on their sum as $4^{N_1+N_2}$. On the other hand, within each species the arguments used to argue the validity of the Dicke basis are still correct so it can be used separately for each species. In particular, the basis for the whole ensemble would be the tensor product of such Dicke state bases. The same results and structure obtained for one-species can be recovered in the bipartite system as well, if the system is initially prepared in a state that is the tensor product of density matrices obtained through the action of collective operators acting on each species separately. If these conditions are met, this leads to a complexity that is the product of the one obtained for one-species separately, and in the case of a bipartite system it reads as $O(N_1^3 \cdot N_2^3)$. Overall, using the tensor product of Dicke basis still allows for an exponential reduction of computational resources.

One particularly interesting physical system is the above described bipartite system but in a driven leaky single mode of a harmonic oscillator. In the most general case where local and collective pumping, dephasing and emission are considered, the master equation reads as follows:

$$\begin{aligned}\dot{\rho} = &-\frac{i}{\hbar}[H^{(1)}_{\mathrm{TLS}} + H^{(2)}_{\mathrm{TLS}} + H_{\mathrm{phot}} + H_{\mathrm{int}}, \rho] \\ &+\frac{w_p}{2}\mathcal{L}_{a^\dagger}[\rho] + \frac{\kappa}{2}\mathcal{L}_{a}[\rho] \\ &+\frac{\gamma^{(1)}_{\Downarrow}}{2}\mathcal{L}_{J^{(1)}_{-}}[\rho] + \frac{\gamma^{(1)}_{\Phi}}{2}\mathcal{L}_{J^{(1)}_{z}}[\rho] + \frac{\gamma^{(1)}_{\Uparrow}}{2}\mathcal{L}_{J^{(1)}_{+}}[\rho] \\ &+\frac{\gamma^{(2)}_{\Downarrow}}{2}\mathcal{L}_{J^{(2)}_{-}}[\rho] + \frac{\gamma^{(2)}_{\Phi}}{2}\mathcal{L}_{J^{(2)}_{z}}[\rho] + \frac{\gamma^{(2)}_{\Uparrow}}{2}\mathcal{L}_{J^{(2)}_{+}}[\rho] \\ &+\sum_{n=1}^{N_1}\frac{\gamma^{(1)}_{\downarrow}}{2}\mathcal{L}_{J^{(1)}_{-,n}}[\rho] + \frac{\gamma^{(1)}_{\phi}}{2}\mathcal{L}_{J^{(1)}_{z,n}}[\rho] + \frac{\gamma^{(1)}_{\uparrow}}{2}\mathcal{L}_{J^{(1)}_{+,n}}[\rho] \\ &+\sum_{n=1}^{N_2}\frac{\gamma^{(2)}_{\downarrow}}{2}\mathcal{L}_{J^{(2)}_{-,n}}[\rho] + \frac{\gamma^{(2)}_{\phi}}{2}\mathcal{L}_{J^{(2)}_{z,n}}[\rho] + \frac{\gamma^{(2)}_{\uparrow}}{2}\mathcal{L}_{J^{(2)}_{+,n}}[\rho]\end{aligned} \tag{14}$$

where $H_{\mathrm{phot}} = \hbar\omega_c a^\dagger a$, κ is the oscillator decay rate, and w_p the pump rate. The interaction Hamiltonian H_{int} can be chosen freely, as long as the permutational invariance for each species is respected. In this project the following interaction Hamiltonian is used:

$$H_{\mathrm{int}} = \hbar g_1(a^\dagger J^{(1)}_+ + a J^{(1)}_-) + \hbar g_2(a^\dagger J^{(2)}_- + a J^{(2)}_+), \tag{15}$$

where g_1 and g_2 are two different coupling constants, one for each species. In the following when referring to the bipartite system, the most general case described in Eq. (14) and Eq. (15) is intended. Relevantly,

in this work the couplings to the two species are set to be explicitly different: $g_2 = 2g_1$. However, other scenarios of interest, as those actually in study in the laboratories, can be readily obtained by properly setting the various rates and by silencing the terms that are not needed.

It is interesting to look at how the block-diagonal density matrix structure obtained for the one-species case is transformed when dealing with a bipartite system. The results are shown in Figure 2b and compared to the one-species case with the corresponding number of TLSs. In particular, it is interesting to note a fractal-like structure of the density matrices in the bipartite case. As a matter of fact, the outer shape of the density matrix (on the right) resembles that of the one-species case (on the left) but the same structure can also be found repeated within the shape itself. In other words, the block-diagonal shape is more fragmented than in the single species case and its found both on the macroscopic and microscopic level. This is a consequence of using as basis the tensor product between two Dicke basis, each of which shows a block-diagonal behaviour as the one in Figure 2a for the reasons explained in section 2.1.2. It is worth reminding that this behaviour is shown only if the initial states are prepared through collective operators only, which is the same assumption made in PIQS for the single species scenario.

3 Equivalence: uncoupled and Dicke basis

In this section the focus is put on providing some ways to test *a posteriori* the equivalence between using the uncoupled basis and the Dicke basis when studying the bipartite system. Firstly, we directly compare the density matrices obtained with each method after the system is let evolve. Secondly, the evolutions in time of the expectation-value of the spin operators obtained in the Dicke basis and the uncoupled basis are compared. Finally, some regularities in the eigenvalues of the density matrices after the evolution in the two basis are found, allowing for a further comparison.

3.1 A simple case: $N = 2$

The most straightforward way to compare the results obtained with the Dicke and uncoupled basis is to compare the density matrices after the evolution. Unfortunately, the Dicke states are laborious to derive and to write explicitly, and so it is the basis change matrix. However, the analysis can be restricted to a simpler case where the matrix can be readily derived and, consequently, results can be compared. This is the case for $N = 2$, which for the bipartite system implies $N_1 = N_2 = 2$. In this case the Dicke basis can be obtained through Eq. (9), which gives the following three states: $|1,1\rangle = |\uparrow,\uparrow\rangle$, $|1,0\rangle = (|\uparrow,\downarrow\rangle + |\downarrow,\uparrow\rangle)/\sqrt{2}$, and $|1,-1\rangle = |\downarrow,\downarrow\rangle$. The fourth state can be obtained by applying the orthonormality condition and is equal to $|0,0\rangle = (|\uparrow,\downarrow\rangle - |\downarrow,\uparrow\rangle)/\sqrt{2}$. This allows to explicitly write the basis change matrix, which in this case maps one Hilbert space to another one of the same dimension. The basis change matrix reads as follows:

$$\begin{pmatrix} 1 & 0 & 0 & 0 \\ 0 & 1/\sqrt{2} & 1/\sqrt{2} & 0 \\ 0 & 0 & 0 & 1 \\ 0 & 1/\sqrt{2} & -1/\sqrt{2} & 0 \end{pmatrix} \tag{16}$$

Consequently, it is possible to transform a density matrix written in the Dicke basis into the uncoupled one, and viceversa. In order to compare the two, the following procedure is followed. Firstly, the initial states are written each in their own basis and are let evolve separately. Secondly, the final density matrices are converted in the same basis; in this case into the Dicke basis. Finally, the two matrices can be compared by taking the relative difference δ_{ij} of each element. The relative difference of the element on the i-th row and j-th column is given by

$$\delta_{ij} = \frac{|z_{ij}^D| - |\tilde{z}_{ij}^U|}{|\tilde{z}_{ij}^U|}, \tag{17}$$

where z_{ij}^D is the element of the density matrix obtained with the Dicke basis whereas $\tilde{z}_{ij}^U$ the one obtained with the uncoupled basis but successively transformed in the Dicke basis. For convenience the absolute value of each element is taken. For the case of two-species the idea is to simply exploit the tensor product between two identical basis change matrices and the overall basis change matrix can be readily obtained. Consequently, it is possible to compare the evolved density matrices for the one-species case (with and without the bosonic coupling) and for the bipartite system (with and without the bosonic coupling). It would be redundant to write here the full matrices of the absolute relative difference but the results can

be summarised by looking at the highest relative difference for each matrix separately. In particular, the relative difference for the case of bipartite system without and with bosonic coupling is equal to $2 \cdot 10^{-8}$ and $1 \cdot 10^{-11}$, respectively. The average relative differences are $5 \cdot 10^{-10}$ and $4 \cdot 10^{-13}$, respectively. Consequently, it can be argued that on average the two methods provide the same results up to 11-13 decimal figures, which means that the results are exactly the same for any practical purpose. The exact process that has been followed can be found on the GitHub repository of the project [17], in the jupyter tutorial `density_matrix_check.ipynb`.

3.2 Expectation-value comparison

In the previous section we have analysed the simple case of 2 TLSs and we have successfully tested the equivalence between the Dicke and uncoupled basis representation, even if as a sanity check it is quite limited. For a more general setting where N can be set to any value, it is possible to compare the expectation-values of spin operators as they are the observables of interest. In particular, the expectation-values can be tested at each time step of the evolution of the two density matrices written in the Dicke and uncoupled basis. This can be readily computed for the bipartite system under study. Specifically, the spin operators used are firstly defined over one-species and then obtained by applying the tensor with the identity acting on the space of the other species: $J^{(1)}_{z/x/y} = J_{z/x/y} \otimes \mathbb{1}^{(2)}$ and $J^{(2)}_{z/x/y} = \mathbb{1}^{(1)} \otimes J_{z/x/y}$. This allows to define operators acting on single species as $J_z^{(1/2)}$, $J_x^{(1/2)}$, and $J_y^{(1/2)}$ or on both species as the sum $J_z^{(1)} + J_z^{(2)}$, $J_x^{(1)} + J_x^{(2)}$, and $J_y^{(1)} + J_y^{(2)}$. The graph obtained for $J_z^{(1)} + J_z^{(2)}$ is illustrated in Figure 3 and shows perfect agreement between PIQS and QuTiP, hence between using the Dicke basis and the uncoupled basis.

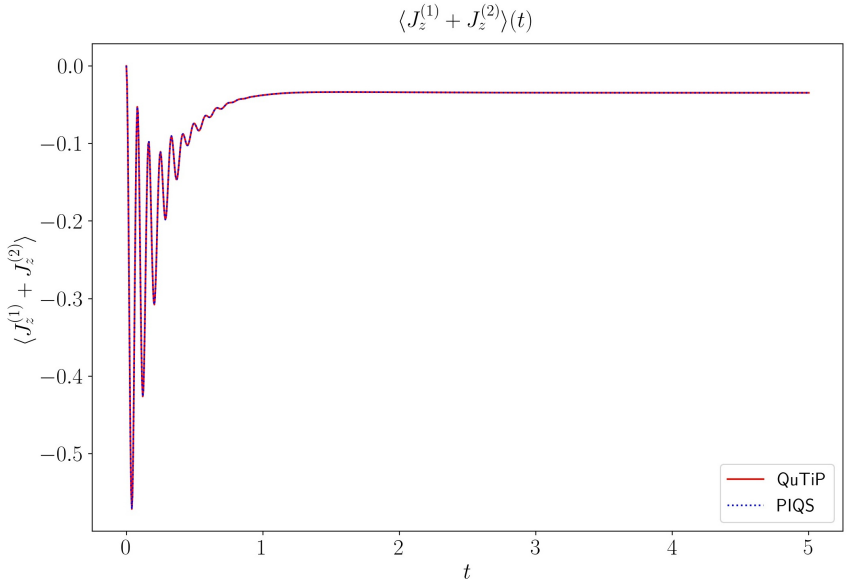

Figure 3: Evolution of the expectation-value of $J_z^{(1)} + J_z^{(2)}$ over time obtained with the Dicke basis (PIQS) and compared with the uncoupled basis (QuTiP). The two lines show perfect agreement as they completely overlap. Relevantly, the couplings to the two species are set to be explicitly different: $g_2 = 2g_1$.

The above analysis is still qualitative though, as overlapping lines may still be characterised by different values up to some decimal place. As in the previous section, one way to obtain a quantitative estimate is to compute the relative differences between the expectation-values obtained with the two different basis at each time step. On average, the relative difference between the two expectation-values is of the order of 10^{-7}, hence negligible. The expectation-values of all the other spin operators considered can be found on the GitHub repository of the project [17], in the jupyter tutorial `j_expectation_check.ipynb`.

3.3 Eigenvalues regularities

We have seen how to test the equivalence of two matrices by writing them in the same basis and by comparing the expectation-values of spin operators. Another possibility is to compare the eigenvalues of the two matrices. In fact, the eigenvalues of a matrix are independent of the basis chosen to represent

them. The comparison is straightforward in the cases where $N = 1$ and $N = 2$, since the dimension of the Hilbert space is the same in both cases ($\mathrm{Dim}(\mathcal{H}) = 1$ and $\mathrm{Dim}(\mathcal{H}) = 4$, respectively), as it can be easily checked through Eq. (10). If $N > 2$ the eigenvalues comparison becomes non trivial since basically the number of eigenvalues of the density matrix represented in the Dicke basis will always be smaller than the one in the uncoupled basis. Consequently, it is not sufficient to simply check whether the eigenvalues are equal up to some decimal figure. Nevertheless, it is still possible to note some regularities between the two sets of eigenvalues.

For $N > 2$ the eigenvalues obtained in the uncoupled basis are not all different, which is instead the case for the Dicke basis. The fact that some eigenvalues obtained with the uncoupled basis are degenerate may be interpreted in the light of the definition of the density matrix itself. For an ensemble of N identical TLSs the density matrix in the uncoupled basis has 2^N basis states and can be diagonalised as $\rho = \sum_{i=1}^{2^N} p_i \left|\phi_i\right\rangle \left\langle\phi_i\right|$. In case there is degeneracy more than one eigenvector may have the same eigenvalue p_i, which is the probability of the system to be in the pure state $\left|\phi_i\right\rangle$. This degeneracy can be interpreted in terms of the permutational symmetry of the system. In fact, if the physical system can be described exactly both in the uncoupled basis and in the Dicke basis, it implies that the degeneracy of the uncoupled basis captures the underlying symmetry of the system. In other words, the eigenvectors associated to the same eigenvalue are overabundant and all the information contained in their eigenvalues may be summarised by simply multiplying each eigenvalue by its multiplicity. This allows to compare the eigenvalues of the density matrices obtained with the uncoupled basis and the Dicke basis, as the total number of eigenvalues would be the same and equal to $n_{\mathrm{DS}}(N)$. In theory this would require identifying identical eigenvalues, count them and sum those that are equal. In practice, eigenvalues are computed numerically and this causes small (but negligible) numerical differences. In order to overcome this problem, one could truncate the eigenvalues obtained at a fixed decimal place and then compare them. This allows to find recurring eigenvalues and to sum their values. This has been done firstly in the simpler case of an ensemble of N identical TLSs. By setting the precision to 7 decimal places, the equivalence of the eigenvalues has been proven for $N \in [1, .., 9]$, considering their multiplicity as described above. Values greater than 9 have not been tested, as on an ordinary computer solving the differential equations in the uncoupled basis for $N = 9$ takes up to 30 minutes already. An illustration of the multiplicity of the eigenvalues in the uncoupled basis for the single species case can be found in Table 1.

Table 1: Comparison between Dicke and uncoupled basis in terms of the number of their states, n_{DS} and n_{US} respectively. When the density matrix is written in the uncoupled basis some eigenvalues occur more than once: the number of occurrences are reported under multiplicity.

N	n_{DS}	n_{US}	Multiplicity
1	2	2	-
2	4	4	-
3	6	8	2,2
4	9	16	3,3,3,2
5	12	32	5,5,4,4,4,4
6	16	64	9,9,9,5,5,5,5,5,5
7	20	128	14,14,14,14,14,14,6,6,6,6,6,6,6
8	25	256	28,28,28,20,20,20,20,20,14,7,7,7,7,7
9	30	512	48,48,48,48,42,42,27,27,27,27,27,27,8,8,8,8,8,8,8,8

Similarly, the eigenvalues have been compared for the case of the bipartite system. Unfortunately, the multiplicity of the eigenvalues has a much more complicated structure, even worsened by the presence of the bosonic coupling. However, it is just as simple to check whether the eigenvalues are equivalent. For a fixed precision of 8 decimal places, the equivalence between the two basis can be tested successfully for various configurations up to $N_1 = N_2 = 3$. As in the one-species scenario, configurations with more TLSs have not been tested due to the uncoupled basis computational constraints. The exact results obtained and the procedure followed is illustrated in the GitHub repository of the project [17], specifically in the dedicated tutorial `eigvals_check.ibynb`. More in depth details about performance comparison between the QuTiP and the PIQS method can be found in the next section.

4 Performance comparison

The key advantage of using the Dicke basis (PIQS method) in place of the uncoupled basis (QuTiP default method) is undoubtedly the computational speedup. In particular, the QuTiP method is viable only for systems with very few TLSs; a rough estimate for a commercial computer would be up to 8 TLSs in the one-species scenario. Obviously, this upper bound is even more limiting for bipartite systems where it applies to the sum of N_1 and N_2. In this section we will investigate what constitutes the main computational bottleneck and compare the performances between QuTiP and PIQS. Specifically, the performance will be compared in the case of one-species ensemble and for the bipartite system, each being considered with and without bosonic coupling.

4.1 Scaling laws

Before actually simulating the systems in the Dicke and uncoupled basis it is useful to estimate the scaling laws that govern the system in the two basis. In particular, this would help investigate the two most computational expensive computations: building the matrices that appear in the master equation and solve the differential equation. These two process constitute the main bottlenecks and will be investigated separately. Nevertheless, the advantage of PIQS with respect to QuTiP is the same in both process and consists in the choice of the Dicke basis, which reduces the overall dimension of the problem. As a matter of fact, when using the uncoupled basis for an ensemble of N TLSs the number of basis elements n_{US} is exponential in N. In particular, the basis contains 2^N states and, as a consequence, a density matrix written in such basis will have 4^N elements. On the other hand, the Dicke basis exploits the permutational invariance of the system already in the choice of the basis, which results in fewer basis states. In particular, an ensemble of N TLSs requires a number of Dicke states n_{DS} given by Eq. (10) which is $O(N^2)$. Consequently, when using the Dicke basis in place of the uncoupled one, the number of basis states decreases from 2^N to $O(N^2)$. Furthermore, Eq. (11) states that the number of non-zero elements of the density matrix scales as $O(N^3)$. Ultimately, when using the Dicke basis in place of the uncoupled basis, the number of ρ elements that must be computed decreases from 4^N to $O(N^3)$.

So far, we have considered that the operators in the master equation can be represented as matrices. This is true also for the Lindblad superoperators $\mathcal{L}$. As a matter of fact, ρ can be treated as a vector and $\mathcal{L}$ as a matrix acting on it. This can be shown by simply applying the map $\rho = \sum_{i,j} p_{ij} |\phi_i\rangle \langle\phi_j| \mapsto |\rho\rangle = \sum_{i,j} p_{ij} |\phi_i\rangle \otimes |\phi_j\rangle$. For instance, the left multiplication superoperator $A\rho$ can be vectorised as $(A \otimes \mathbb{1}) |\rho\rangle$. The Lindblad operator is thus represented as a $d^2 \times d^2$ matrix, d being the dimension of the basis and d^2 the number of elements in ρ. This allows to express the scaling laws for the dimension of the matrices that describe the problem. The scaling laws for the one-species scenario are reported in Table 2 while those for the bipartite system in Table 3.

Table 2: Scaling laws for an ensemble of N single species TLSs without and with bosonic coupling (n photons).

		One-species (N TLS)	+ bosonic coupling (n photons)
QuTiP	basis dim	2^N	$2^N \cdot n$
	ρ elements	4^N	$4^N \cdot n^2$
	$\mathcal{L}$ dim	4^N	$4^N \cdot n^2$
PIQS	basis dim	$O(N^2)$	$O(N^2 \cdot n)$
	ρ elements	$O(N^3)$	$O(N^3 \cdot n^2)$
	$\mathcal{L}$ dim	$O(N^4)$	$O(N^4 \cdot n^2)$

Table 3: Scaling laws for an ensemble of N_1 TLSs of one-species and N_2 TLSs of another species without and with bosonic coupling (n photons).

		Two-species (N_1, N_2 TLSs)	+ bosonic coupling (n photons)
QuTiP	basis dim	$2^{N_1+N_2}$	$2^{N_1+N_2} \cdot n$
	ρ elements	$4^{N_1+N_2}$	$4^{N_1+N_2} \cdot n^2$
	$\mathcal{L}$ dim	$4^{N_1+N_2}$	$4^{N_1+N_2} \cdot n^2$
PIQS	basis dim	$O(N_1^2 \cdot N_2^2)$	$O(N_1^2 \cdot N_2^2 \cdot n)$
	ρ elements	$O(N_1^3 \cdot N_2^3)$	$O(N_1^3 \cdot N_2^3 \cdot n^2)$
	$\mathcal{L}$ dim	$O(N_1^4 \cdot N_2^4)$	$O(N_1^4 \cdot N_2^4 \cdot n^2)$

The PIQS method can be extended to the case of multiple species as well. In case two-species are considered, it is possible to represent each of them separately in the Dicke basis and then to compute the tensor product between the two basis. The scaling laws obtained for the case of two-species are reported in Table 3. In both cases it can be noted that the PIQS method provides an exponential speedup in the computational complexity. It is more apparent in the case without bosonic coupling since the additional n dimensions increase both QuTiP and PIQS complexity in the same way. In other words, the computational speedup obtained through the Dicke basis cannot be applied for the bosonic terms. Nevertheless, as will be shown in the next section, PIQS is still considerably faster.

4.2 Runtime comparison

At this point it is possible to compare the performances of PIQS and QuTiP both for the single species and the bipartite system. In particular, the single species case is let evolve according to the dynamics expressed by Eq. (1) while the bipartite system by Eq. (13). The bosonic coupling term can be readily added in both cases as in Eq. (14). The specific parameters and rates used in the simulations are not relevant to the computational complexity of the problem, but more details may be found in the GitHub repository of the code [17] under the folder `results`.

The idea behind the simulation is simply to let the computer first build the system matrices and then solve the differential equation. The variable of interest is the runtime as a function of the dimension of the system, which is expressed in terms of the number N of identical TLSs that compose the system. The runtime can be easily plotted and compared between QuTiP and PIQS and is illustrated separately for the time taken to build the matrix and the time needed to solve the differential equation. Note that the second include the first since, in order to solve the problem, it is necessary to first build it. It could be argued that one could plot the difference in order to isolate the computational complexity of solving the differential equation. Actually, it is also true that in practice the user is interested in using the method fully so the total time required is of greater interest. For the sake of the illustration, the runtime taken for building the system and to solve the differential equation are reported in two different sections.

4.2.1 Building the matrices

As anticipated, the first computationally intensive operation is to build the matrices that compose the master equation. In Figure 4 the comparison between the one-species scenario and the bipartite system in terms of runtime is illustrated. In particular, the graph underlines the difference between using the uncoupled basis with QuTiP and the Dicke basis with PIQS between the one-species scenario and the bipartite system.

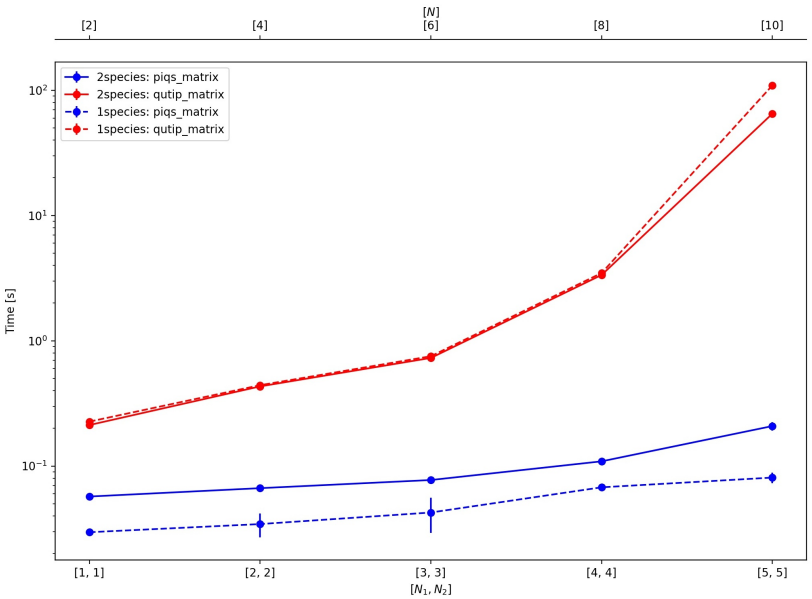

Figure 4: Runtime taken for building the master equation matrices with QuTiP (red line) and with PIQS (blue line). The one-species scenario ($[N]$, dashed line) is compared with the bipartite system ($[N_1, N_2]$, solid line), both without the bosonic coupling.

It is apparent that when using the uncoupled basis the complexity required for the single species case and for the bipartite system is the same. As a matter of fact, from Table 2 and 3 the scaling law for the matrices $\mathcal{L}$ read as 4^N and $4^{N_1+N_2}$ for the one-species case and the bipartite system, respectively. In Figure 4 the axes have been positioned so that $N_1 + N_2 = N$, which results in the exact same complexity for QuTiP. In contrast, when using PIQS the single species case and the bipartite system are characterised by a complexity of $O(N^4)$ and $O(N_1^4 \cdot N_2^4)$, respectively. Furthermore, it is interesting to note that in the case of a bipartite system the complexity is influenced by the sum $N_1 + N_2$ in QuTiP and by the product $N_1 \cdot N_2$ in PIQS. This means that in QuTiP having any combination $N_1 + N_2 = N$ makes no difference whereas in PIQS the most efficient one is $1 \cdot (N-1)$ and the most inefficient one is $N/2 \cdot N/2$. This may be a valuable piece of information when dealing with the PIQS method for bipartite systems, but also multi-species scenario as will be argued in the following paragraphs.

It is also interesting to compare the runtime for building the matrices for the bipartite system and compare the cases with and without the bosonic coupling. As reported in Table 3 the scaling factor added by n photons causes the complexity to grow by a factor of n^2 in both QuTiP and PIQS. This can be clearly seen in Figure 5. Specifically, no or little difference is observed for the cases of $n = 1$ and $n = 2$ both in QuTiP and PIQS. As soon as n increases though, the runtime increases as well. This behaviour has the same magnitude in QuTiP and PIQS, confirming what is expected from the scaling laws.

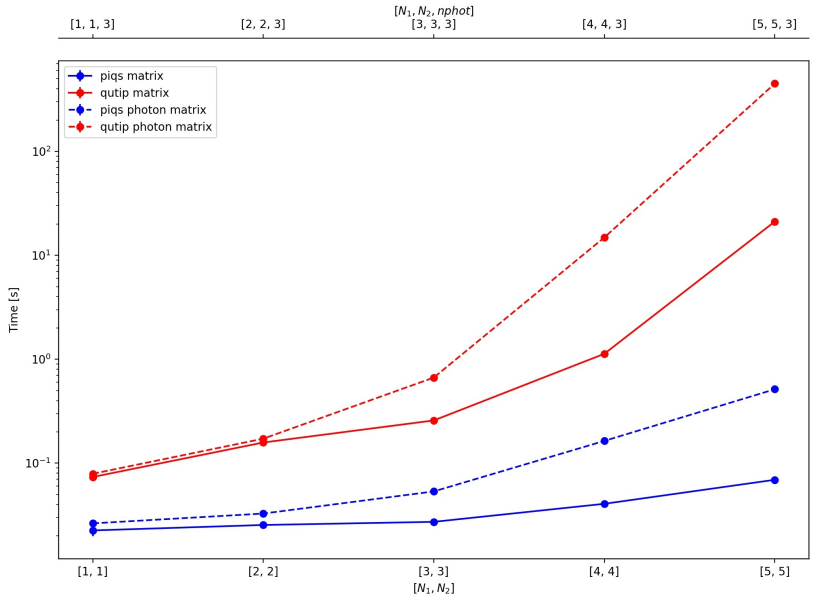

Figure 5: Runtime taken for building the master equation matrices with QuTiP (red line) and with PIQS (blue line). The bipartite system scenario without bosonic coupling ($[N_1, N_2]$, dashed line) is compared with the addition of bosonic coupling ($[N_1, N_2, nphot]$, solid line).

4.2.2 Solving the differential equations

It has been argued that the dimension of the Hilbert space and of the matrices in the master equation are clearly influenced by the dimension of the basis used. Furthermore, the dimension of the basis determines the number of elements of the density matrix that must be computed when solving the differential master equation. As a consequence, the most relevant parameter, when analysing the complexity of solving the differential master equation, is the number of elements in the density matrix. In particular, in the one-species scenario the number of elements scales as 4^N in the uncoupled basis and as $O(N^3)$ in the Dicke basis. Similarly, in the bipartite system the scaling laws are $4^{N_1+N_2}$ and $O(N_1^3 \cdot N_2^3)$ for QuTiP and PIQS, respectively. The corresponding runtime obtained experimentally are reported in Figure 6.

Similarly to what observed in Figure 4, the runtime required for the single species case and the bipartite system is identical when the QuTiP method is used. In fact, as long as $N_1 + N_2 = N$ the complexity of the bipartite system and the one of the single species give the same results. In contrast, with PIQS the scaling laws are $O((N_1 + N_2)^3)$ in the single species case and $O(N_1^3 \cdot N_2^3)$ in the bipartite system. It is true in this case as well that QuTiP requires the same computational complexity at fixed N, regardless of N_1 and N_2, whereas PIQS is faster when N_1 and N_2 are close to 1 and $N_1 + N_2 - 1$, or in other words

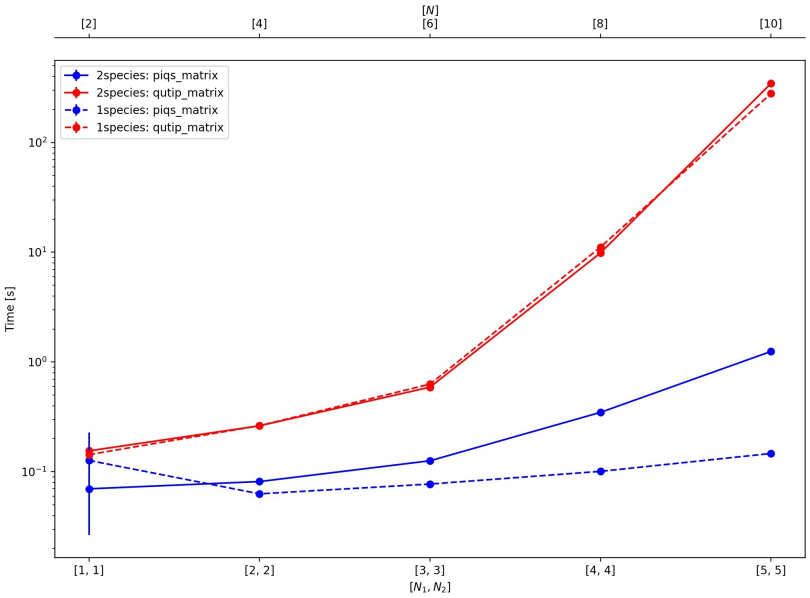

Figure 6: Runtime taken for solving the differential master equation with QuTiP (red line) and with PIQS (blue line). The one-species scenario ($[N]$, dashed line) is compared with the bipartite system ($[N_1, N_2]$, solid line), both without the bosonic coupling.

when the difference $N_1 - N_2$ is large. The initial intersection between the two PIQS curves seems to be in contradiction with the scaling laws, which state that the complexity increases with the number of TLSs. Actually, if the uncertainty associated to the results is considered, the two measures are compatible. The uncertainty is simply obtained as the standard deviation between two measurements of runtime; some points don't show an error bar only because is too small to be visible. The observations are indeed compatible with the predictions.

Predictions are confirmed also when comparing the bipartite system for the configurations with and without the bosonic coupling, as shown in Figure 7. In particular, the multiplicative factor of n^2 affects QuTiP and PIQS in the same way as they both show a proportional increase in the runtime. It is also interesting to note that such increase can be quite significant for some configurations. For instance, the bipartite system with bosonic coupling takes more time to be solved in PIQS with respect to the bipartite system without bosonic coupling with QuTiP. This is true only for configurations smaller than $[4, 4]$ since, when more TLSs are introduced in the system, the exponential complexity of QuTiP takes over PIQS's. However, it is worth underlying that the comparison is being made between a more complex system (with bosonic coupling) in PIQS with a simpler one (without bosonic coupling) in QuTiP. What is interesting is that the intersection between the two curves is expected by the scaling laws in Table 3: $4^{N_1+N_2}$ and $O((N_1 + N_2)^3 \cdot n^2)$, respectively. In fact, it is sufficient to substitute the numbers for the configurations $[4, 4]$ vs. $[4, 4, 3]$ and $[5, 5]$ vs. $[5, 5, 3]$ to see that QuTiP complexity takes over PIQS's.

Overall, the PIQS method has proved to be faster than the QuTiP both in building the matrices and in solving the differential equations. This was true both for the single species ensemble and it still is for the bipartite system. Even when bosonic couplings are added, PIQS is faster compared to QuTiP and its faster even compared to QuTiP without bosonic coupling, for sufficiently large ensemble ($N = N_1 + N_2 > 8$). Particularly relevant is the analysis of the contribution to the complexity of N_1 and N_2. As a matter of fact, the scaling laws obtained in Table 2 can be readily generalised to the case of arbitrarily many mixed-species. By having understood how N_1 and N_2 influence the complexity, one can estimate in a more general case with d species how the configuration of each $N_1, N_2, N_3, ..., N_d$ affects the overall complexity. In particular, QuTiP complexity scales exponentially with the sum $4^{N_1+N_2+...+N_d}$ while PIQS polynomially as $N_1^3 \cdot N_2^3 \cdot ... \cdot N_d^3$.

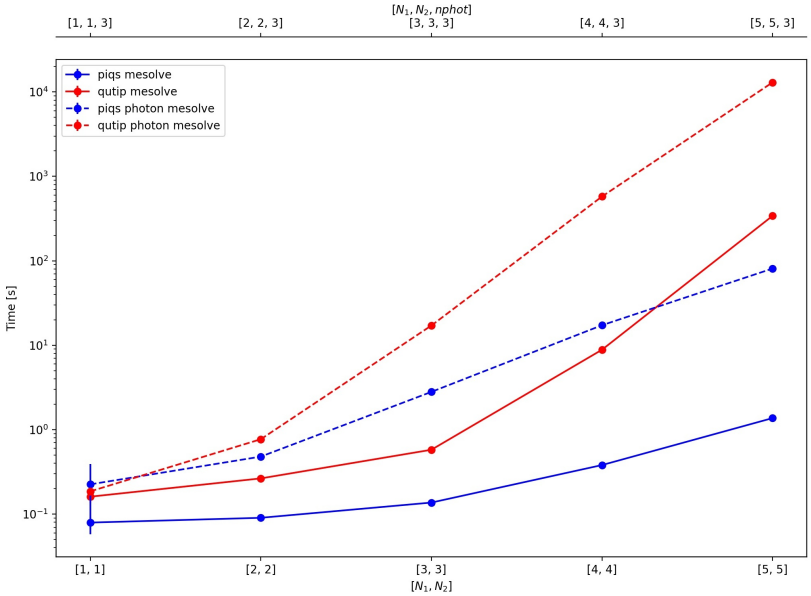

Figure 7: Runtime taken for solving the differential master equation with QuTiP (red line) and with PIQS (blue line). The bipartite system scenario without bosonic coupling ($[N_1, N_2]$, dashed line) is compared with the addition of bosonic coupling ($[N_1, N_2, nphot]$, solid line).

5 Conclusions

In this work we have demonstrated the possibility to exploit the concepts used in the PIQS library in the single species scenario for a more complex system involving two-species of TLSs. The original permutational invariance is translated into partial permutational symmetry and this allows to efficiently simulate the dynamics of a bipartite system. The standard QuTiP method requires exponential resources in the number on TLSs while the generalized PIQS method has a polynomial complexity. Firstly, the equivalence between QuTiP and PIQS has been validated *a posteriori* in three independent ways by comparing expectation-values, density matrices elements and common eigenvalues. Secondly, the performance of the QuTiP and PIQS method has been investigated in terms of the runtime required to build the matrices and to solve the master equation. In both cases PIQS proved to allow for a significant reduction in the computational resources for the bipartite system as well. Results have been reported as a function of the number of TLSs of each species N_1 and N_2, allowing to make predictions for a more general mixed-species scenario, which may be extended according to the physical system under study.

References

[1] Klaus Hepp and Elliott H Lieb. "On the superradiant phase transition for molecules in a quantized radiation field: the dicke maser model". In: *Annals of Physics* 76.2 (1973), pp. 360–404. ISSN: 0003-4916. DOI: https://doi.org/10.1016/0003-4916(73)90039-0. URL: http://www.sciencedirect.com/science/article/pii/0003491673900390.

[2] Nathan Shammah et al. "Open quantum systems with local and collective incoherent processes: Efficient numerical simulations using permutational invariance". In: *Physical Review A* 98.6 (Dec. 2018). ISSN: 2469-9934. DOI: 10.1103/physreva.98.063815. URL: http://dx.doi.org/10.1103/PhysRevA.98.063815.

[3] J.R. Johansson, P.D. Nation, and Franco Nori. "QuTiP: An open-source Python framework for the dynamics of open quantum systems". In: *Computer Physics Communications* 183.8 (2012), pp. 1760–1772. ISSN: 0010-4655. DOI: https://doi.org/10.1016/j.cpc.2012.02.021. URL: http://www.sciencedirect.com/science/article/pii/S0010465512000835.

[4] Michael Gegg and Marten Richter. "PsiQuaSP–A library for efficient computation of symmetric open quantum systems". In: *Scientific Reports* 7.1 (Nov. 2017). ISSN: 2045-2322. DOI: 10.1038/s41598-017-16178-8. URL: http://dx.doi.org/10.1038/s41598-017-16178-8.

[5] R. H. Dicke. "Coherence in Spontaneous Radiation Processes". In: *Phys. Rev.* 93 (1 Jan. 1954), pp. 99–110. DOI: 10.1103/PhysRev.93.99. URL: https://link.aps.org/doi/10.1103/PhysRev.93.99.

[6] D. Meiser and M. J. Holland. "Steady-state superradiance with alkaline-earth-metal atoms". In: *Phys. Rev. A* 81 (3 Mar. 2010), p. 033847. DOI: 10.1103/PhysRevA.81.033847. URL: https://link.aps.org/doi/10.1103/PhysRevA.81.033847.

[7] Masahiro Kitagawa and Masahito Ueda. "Squeezed spin states". In: *Phys. Rev. A* 47 (6 June 1993), pp. 5138–5143. DOI: 10.1103/PhysRevA.47.5138. URL: https://link.aps.org/doi/10.1103/PhysRevA.47.5138.

[8] Peter Kirton et al. "Introduction to the Dicke Model: From Equilibrium to Nonequilibrium, and Vice Versa". In: *Advanced Quantum Technologies* 2.1-2 (2019), p. 1800043. DOI: https://doi.org/10.1002/qute.201800043. eprint: https://onlinelibrary.wiley.com/doi/pdf/10.1002/qute.201800043. URL: https://onlinelibrary.wiley.com/doi/abs/10.1002/qute.201800043.

[9] S. Ashhab and Franco Nori. "Qubit-oscillator systems in the ultrastrong-coupling regime and their potential for preparing nonclassical states". In: *Phys. Rev. A* 81 (4 Apr. 2010), p. 042311. DOI: 10.1103/PhysRevA.81.042311. URL: https://link.aps.org/doi/10.1103/PhysRevA.81.042311.

[10] N. Shammah and S. Ahmed. *PIQS*. https://github.com/nathanshammah/piqs. 2018.

[11] Yusuke Hama, William J. Munro, and Kae Nemoto. "Relaxation to Negative Temperatures in Double Domain Systems". In: *Phys. Rev. Lett.* 120 (6 Feb. 2018), p. 060403. DOI: 10.1103/PhysRevLett.120.060403. URL: https://link.aps.org/doi/10.1103/PhysRevLett.120.060403.

[12] Minghui Xu et al. "Synchronization of Two Ensembles of Atoms". In: *Phys. Rev. Lett.* 113 (15 Oct. 2014), p. 154101. DOI: 10.1103/PhysRevLett.113.154101. URL: https://link.aps.org/doi/10.1103/PhysRevLett.113.154101.

[13] V. Negnevitsky et al. "Repeated multi-qubit readout and feedback with a mixed-species trapped-ion register". In: *Nature* 563.7732 (Nov. 2018), pp. 527–531. ISSN: 1476-4687. DOI: 10.1038/s41586-018-0668-z. URL: http://dx.doi.org/10.1038/s41586-018-0668-z.

[14] Jonathan P. Home. *Quantum science and metrology with mixed-species ion chains*. 2013. arXiv: 1306.5950 [quant-ph].

[15] Michael Gegg. "Identical emitters, collective effects and dissipation in quantum optics : novel numerical approaches for quantum master equations". Doctoral Thesis. Berlin: Technische Universität Berlin, 2017. DOI: 10.14279/depositonce-6526. URL: http://dx.doi.org/10.14279/depositonce-6526.

[16] Leonard Mandel and Emil Wolf. *Optical Coherence and Quantum Optics*. Cambridge University Press, 1995. DOI: 10.1017/CBO9781139644105.

[17] Marcello Negri. *BipartiteQuantumSystems*. https://github.com/marcello-negri/BipartiteQuantumSystems. 2020.